Heliyon 10 (2024) e24707

Contents lists available at ScienceDirect

Heliyon

journal homepage: www.cell.com/heliyon

Research article

Mechanism and kinetic of piezo-catalytic desulfurization of model and actual fuel samples over Ce_xO_y/SrO nanocomposite at room temperature

Karwan M. Rahman [a], Omid Amiri [b,*], Sangar S. Ahmed [a], Savana J. Ismael [a], Noor S. Rasul [a], Karukh A. Babakrb [d], Mahnaz Dadkhah [c], Mohammed A. Jamal [d]

[a] Chemistry Department, College of Science, Salahaddin University, Kirkuk Road, 44001, Erbil, Kurdistan Region, Iraq
[b] Department of Medical Biochemical Analysis, Cihan University-Erbil, Kurdistan Region, Iraq
[c] Department of Chemistry, University of Adelaide, Adelaide, SA 5005, Australia
[d] Department of Petroleum and Mining Engineering, Faculty of Engineering, Tishk International University, Erbil, Iraq

ARTICLE INFO

Keywords:
Piezo-desulfurization
Model fuel
Kerosene
Ce_xO_y/SrO nanocomposite
Piezo

ABSTRACT

SO_x emissions are primarily caused by compounds containing sulfur in petroleum and fuels, which lead to severe air pollution. For this reason, it is necessary to develop a fast and simple desulfurization method in order to comply with ever-increasing environmental regulations. The newly discovered piezo-catalyst nanocomposite Ce_xO_y/SrO can convert mechanical energy directly into chemical energy, thereby enabling mechanically oxidative sulfur desulfurization. 320 W of bath sonication were used to polarize and activate the prepared piezo-catalyst nanocomposite Ce_xO_y/SrO for sulfur removal from thiophene and dibenzothiophene as model fuels and kerosene as a real fuel. Using uniform and spherical CeO_2/SrO nanocomposites resulted in the highest desulfurization rates of 95.4 %, 97.3 %, and 59.7 %, respectively, for thiophene and dibenzothiophene. This study examined the effect of several parameters, such as sulfur concentration, pH of fuel, dosage of CexOy/SrO nanocomposite, power and time of ultrasonic, and shaking time, on the piezo-desulfurization of thiophene (TP) and dibenzothiophene (DBTP). To identify the major active species in piezo desulfurization, radical trapping experiments were conducted. This study investigated the possibility of reusing the catalyst, and the piezo-desulfurization activity that was demonstrated in the removal of TP and DBTP after 11 cycles as well as the ability of the catalyst to remove real fuel even after 14 cycles was promising. As the kinetic results show, the reaction follows the second order with K = 0.0050. Also, thermodynamic results showed the oxidation of sulfide to sulfoxide and sulfoxide is endothermic. Activation energy for second order rate constant is (3.824 Kj/mole). 0.0236 mol^{-1}. Sec^{-1} was calculated for Arrhenius Constant.

1. Introduction

Today, the most significant issues and challenges are environmental limitations and restrictions mainly relating to fuel quality and eliminating obstinate sulfur complexes from fuel refining in modern companies themselves, as well as the most expensive ones. Fuels

* Corresponding author.
E-mail addresses: o.amiri1@gmail.com, omid.amiri@cihanuniversity.edu.iq (O. Amiri).

https://doi.org/10.1016/j.heliyon.2024.e24707
Received 15 March 2023; Received in revised form 27 December 2023; Accepted 12 January 2024
Available online 18 January 2024

containing high levels of sulfur complexes contribute significantly to air pollution through SOx emissions. Acid rain and the decadence of human health are a result of the reduction and emission of sulfur oxide resources. Therefore, researchers have been focusing on reducing the determined sulfur content of fuels in order to minimize or improve this content [1,2] (see Scheme 1).

Natural petroleum contains a variety of organosulfur compounds, including aromatic types such as thiophene (C_4H_4S), which are inert and do not react, resulting in common contamination and impurity as a transportation fuel. In addition to being very similar to benzene, heterocyclic thiophene is also a fairly simple molecule. It is therefore an ideal chemical model for studying the catalytic C–S bond. In the thiophene molecule, there are two sets of electrons located on its S atom, with one set situated in the six-electron system and the other set in the ring's plane. Thiophene can function as an n-type donor by shifting the electron pair from the S atom to a surface cation or as a π-type donor by utilizing the delocalized electrons in the aromatic ring to create a π-complex with the cation [3].

As shown in Fig. 1, various methods of desulfurization have been reported so far to remove sulfur, including hydro-desulfurization, oxidative desulfurization [4,5] bio-desulfurization [6,7] alkylation-based desulfurization [8,9] chlorinolysis-based desulfurization [10,11] and other methods [12–14]. This study demonstrates the operation of an oxidative desulfurization procedure utilizing a novel piezo-catalyst nanocomposite. The original method of oxidative desulfurization involved the reaction of sulfur with an oxidizing agent, such as H_2O_2. In oxidative desulfurization, two steps are involved. Through the oxidation of sulfur-containing molecules, sulfur compounds are transformed into their corresponding sulfones or sulfoxides. Following the removal of oxidized sulfur compounds from the system, the elimination properties of oxidized sulfur compounds are compared with those of non-oxidized sulfur compounds. One of the most compelling advantages of this study is the fact that sulfur-containing molecules can be oxidized both in model fuel and real fuel at room low temperature (30 ± 2 °C) and simply by using a piezo-catalytic effect to oxidize and change sulfur into a form that can be removed from the fuel. Piezo-catalytic materials exhibit catalytic activity when subjected to external mechanical distortions [15]. According to Hong et al. [16], the first direct conversion of mechanical energy into chemical energy was performed by splitting water for piezoelectric microfibers in 2010. As piezoelectric catalysis has gained in popularity over the past few years, it has also attracted more attention in the areas of energy conversion and environmental and ecological remediation [15,17–23]. It was evident from the results of the desulfurization process that nano-composites were extremely effective at removing sulfur compounds. A desulfurization procedure was carried out under ambient conditions, and the effects of changing pH, shaking time, and ultrasonic time and power were examined for these specific nano-composites. Lastly, a study of the mechanism and kinetics behind the desulfurization method by using prepared piezo catalysts was conducted. SrO, CeO_2, and Ce_2O_3 (Ce_xO_y/SrO) nanocomposites have been prepared by a microwave method as an efficient piezo catalyst for the desulfurization of model fuel and real fuel. There was a significant effect of synthesis

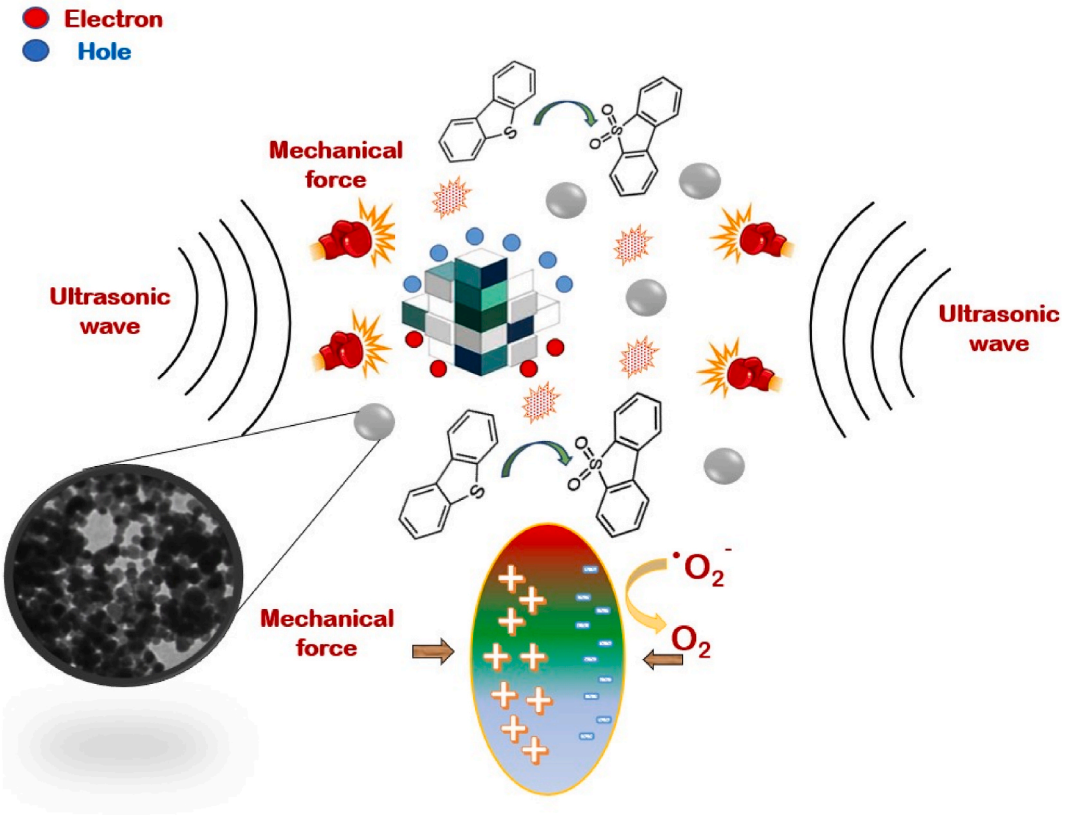

Scheme 1. Supposable piezo-desulfurization mechanism under external mechanical force provided by ultrasonic vibration by prepared CexOx/SrO Nano-composite.

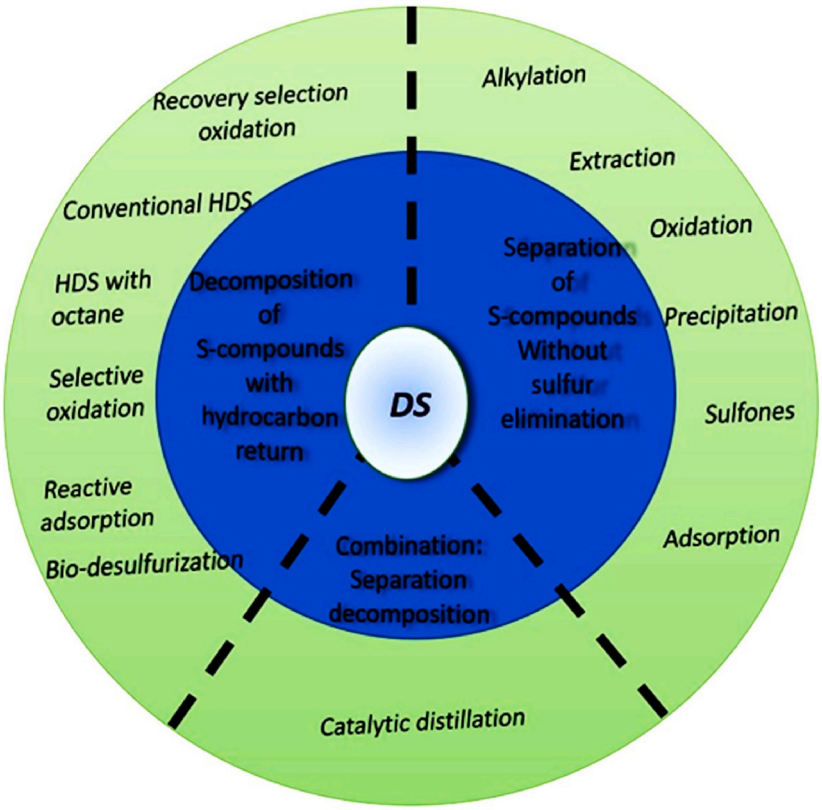

Fig. 1. Different methods were used for desulfurization of fuel.

parameters such as microwave time, power, and calcination temperature on the morphology and composition of Ce_xO_y/SrO nanocomposites. The synthesis parameters were adjusted in order to produce Ce_xO_y/SrO nanocomposites with different morphologies and piezo catalytic activities. The use of CeO_2/SrO nanocomposite with spherical morphology resulted in the removal of 97.3 % of sulfur.

2. Experimental

2.1. Material

$Sr(NO_3)_2{\cdot}2H_2O$ (99.9 %), $Ce(NO_3)_3{\cdot}6H_2O$ (99.9 %) and sodium dodecylbenzene sulfonate (99.9 %) were purchased from Fluka. Ethylenediaminetetraacetic acid disodium (EDTA-2Na, 99.9 %) and ethanol were purchased from BDH Chemicals (England). 1, 4-benzoquinone (BQ, 99.9 %), and Isopropanol (IPA, 99.9 %) were purchased from Scharlau (Spain). Sodium dodecylbenzene sulfonate (SDS, 99.9 %) and ammonium hydroxide were purchased from Sigma-Aldrich and Merch, respectively. Thiophene and

Table 1
Principal physical characters of kerosene.

No	Test description		Unit	Test Method	Results
1	Flash point		°C	ASTM D93	43
2	Specific Gravity@15.5°C		–	ASTM D1217	0.7828
3	API Gravity		–	ASTM D287	49.26
4	Kinematic Viscosity @40 °C		mm^2/sec	ASTM D445	1.21
5	Water content		vol%	ASTM E203	0.0
6	Initial Boiling Point, IBP		°C	ASTM D86	130
7	Distillation temperature	10 % Recovered, vol%	°C		154
8		50 % Recovered, vol%			196
		90 % Recovered, vol%			228
	Final Boiling Point, FBP		°C		254
9	Recovered		vol%		97.0
10	Evaporated		vol%		1.0
11	Residue		vol%		2.0
12	Total Sulfur Content		mass%	ASTM D4294	0.2023

dibenzothiophene and raw kerosene as a real fuel in this study, was taken from a local Company, and Table 1 shows the chief physical characters of raw kerosene.

2.2. Synthesis and characterization of SrO and Ce_2O_3 nano-composites Piezo catalyst

In the first step, 20 mL of a mixture of distilled water and methanol were prepared in a 2:1 ratio, with the addition of 0.08 mM Sr $(NO_3)_2$ (Solution A) and $Ce(NO_3)_3$ (solution B) in up to 10 mL of each solution. After that, the above solutions were mixed. Afterward, 5 mL of 0.016 mM SDS aqueous solution was added slowly to the mixture of A and B. SDS is a surfactant that helps to control the shape and size of products. When the mixture is ready, add 10 mL of 2 mM NaOH dropwise to the mixture solution to adjust the pH. Microwave the mixture for 3 min (30 s on, 60 s off). We then washed it with ethanol, dried it, and calcined it at 550 °C for 5 h in a muffle furnace (HERBERT, West Germany). A list of piezo-catalysts prepared with different parameters is given in Table 2, where the prepared catalysts are labeled as C1–C15.

2.3. Applying piezo catalyst for desulfurization process

Following the successful synthesis of the nano-composites, the synthesized piezo catalysts were applied for the oxidative desulfurization of the model and real fuel. TP or DBTP/n-hexane solution with a sulfur content of 500 ppm and real fuel was mixed with 50 mg of piezocatalyst, and a Pyrex cell was used to perform the piezo reaction. Piezo-desulfurization was achieved using an ultrasonic bath of a 20 kHz ultrasonic device with a maximum output power of 360 W. Prior to running the piezo-desulfurization process, the samples were stirred in the dark for 30 min. It is imperative to establish an equilibrium phase between adsorption and desorption during this step. At each time interval, 10 mL of desulfurized samples were withdrawn and centrifuged for 10 min at 6000 rpm. By adding ice cubes and frequently changing the water, we maintain the temperature in the ultrasonic bath. Following the removal of the precipitate, the oxidized sulfur compounds were extracted using a one-to-one volume ratio of DMF. DMF is a polar (hydrophilic) aprotic solvent that is commonly used to extract polar organosulfur compounds. The solution was separated by magnetic stirring for 15 min at room temperature. The fuel's desulfurization efficiency (DS) was calculated using the formula (eq. (1)) after separating two phases from DMF and hexane, where the model fuel was found in the top phase and analyzed using an X-ray sulfur meter.

$$DS\% = ((A0\text{-}At)/A0)*100 \quad (1)$$

Where A0 and At are the concentrations of sulfur in the fuel solution for initial and after t times, respectively [24]. Furthermore, a designed experiment has been performed for radical trapping to be able to explain the main active types and species in the piezo desulfurization process. The process of piezo desulfurization refers to the removal of sulfur through the use of piezo catalysts. The experimental method was identical for all piezo-desulfurization tests. Free radical scavenger experiment was used by using different types of scavengers, including Na_2-EDTA (as a quencher of h+), IPA (as a quencher of OH), and *para*-Benzoquinone (BQ) (as a quencher of $^{\cdot}O_2^-$) [25,26].

2.4. Characterization techniques

In order to investigate the crystal structure of the samples, an X-ray diffractometer (Philips X'pert Pro MPD, The Netherlands) was equipped with Ni-filtered Cu Kα radiation (λ = 1.54 Å). A X-Max Oxford, England, was used to perform the EDS (energy dispersion spectroscopy) analysis. ΣIGMA/VP- ZEISS, Germany was used to recording FESEM images. TEM images were captured by means of transmission electron microscopy (TEM, Zeiss). Total sulfur content of fuels was analyzed by utilizing an X-ray sulfur meter, RX360SH, Tanaka, Japan.

Table 2
Experimental Details of conditions for synthesis of CexOx/SrO Nano-composites.

Sample	Microwave power (W)	Microwave time (m)	Cycle pulse time	Calcination Temperature (°C)	Calcination Time (h)
C1	600	3	30s on 60s off	550	5
C3	600	3	30s on 15s off	550	5
C4	700	3	30s on 60s off	550	5
C5	700	3	30s on 30s off	550	5
C6	700	3	30s on 10s off	550	5
C7	900	3	30s on 60s off	550	5
C10	700	4	30 s on 60s off	550	5
C11	700	6	30s on 60s off	550	5
C12	700	4	30 s on 60 s off	400	5
C13	700	4	30s on 60s off	700	5
C14	700	4	30s on 60s off	550	3
C15	700	4	30s on 60s off	550	7

3. Results and discussion

3.1. Characterization of as-prepared piezo catalysts

Using a simple and time-saving microwave technique, Ce_xO_y/SrO nanocomposites have been synthesized in this research. In comparison with conventional heating methods, microwave-based methods for the synthesis of catalysts offer several advantages. The following are some of the advantages of synthesizing catalysts using microwave irradiation: accelerated reaction rates: microwave irradiation can rapidly heat the reactants and catalyst, thereby accelerating the rate of reaction. As a result of microwaves' selective heating effect, temperature gradients can be precisely controlled, allowing for efficient activation of catalysts and a reduction in reaction times. In industrial processes, this acceleration can result in significant increases in productivity and throughput. As opposed to conventional heating methods, microwave methods can provide energy-efficient synthesis processes. By directly heating the reaction mixture, microwaves minimize heat loss to the surrounding environment. As a result of this focused energy transfer, energy consumption is reduced and reaction times are shortened, which results in cost savings and environmental benefits. In comparison with conventional methods, microwave heating can often allow reactions to take place under milder conditions. This can reduce the need for harsh reaction conditions, such as high temperatures or pressures, resulting in improved safety and compatibility with sensitive reactants or functional groups.

Ce_xO_y/SrO nanocomposites are capable of acting as piezo-catalysts since they can release electrons and holes upon exposure to mechanical forces or local vibrations. Several methods can be used to provide external mechanical energy to activate piezo-catalysts, including vortex-induced shearing, ultrasonic cavitation, and physical bending [27,28]. In this study, ultrasonic power was applied to transfer mechanical force to activate Ce_xO_y/SrO nanocomposites for sulfur removal at room temperature. The very first step was to consider the effects of different microwave synthesis parameters, including microwave power, microwave time, and pulse cycling. As-prepared nanocomposites must be calcined to transform from an amorphous to a crystalline state. As a result, the effects of calcination time and temperature have also been considered.

Various techniques were employed to characterize the as-prepared Ce_xO_y/SrO nanocomposites. According to Fig. 2a, the XRD

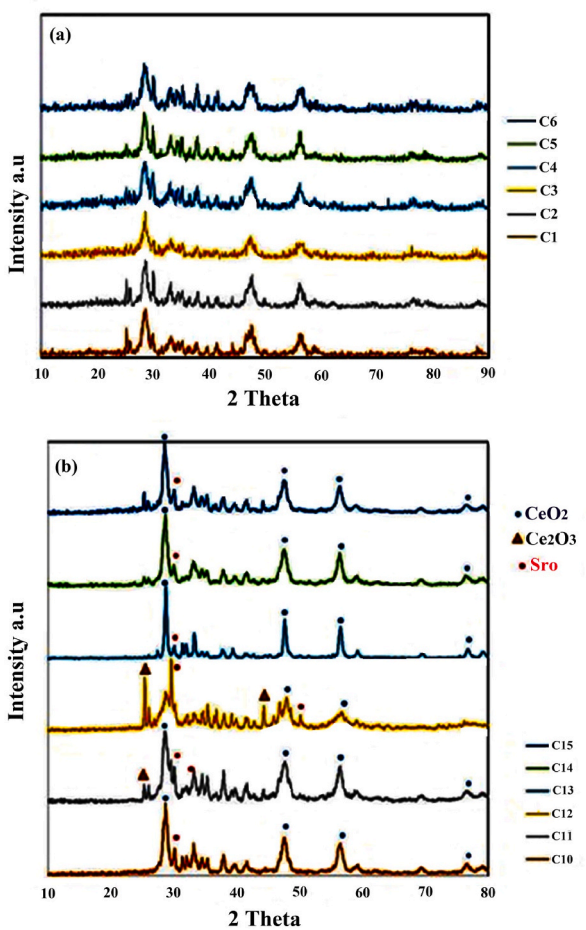

Fig. 2. A) XRD pattern of C1–C6 and b) XRD pattern of C10–C15.

patterns for C1 to C6 indicate that the microwave time of 3 min was not sufficient to prepare uniform nanocomposites. The SEM images confirm the reason for the broad XRD pattern. Ce_xO_y/SrO nanocomposites were successfully synthesized by increasing the microwave time. A summary of the XRD patterns of C10 to C15 is shown in Fig. 2b, and the characteristic peak related to CeO_2 can be observed in all samples except C12. Accordingly, sample C12 was calcined at 400 °C, which confirmed that this temperature was insufficient to convert Ce_2O_3 into CeO_2. XRD results indicate that the successfully prepared samples contain a mixture of CeO_2 and SrO. A cubic phase of CeO_2 or cerianite has been discovered in C10, C11, C13, C14, and C15 with the reference code 96-900-9009. It has been found that all of the samples from C10 to C15 contain SrO with reference code 96-710-2431 and cubic phase. The SEM images of samples C1–C7 are shown in Fig. 3 a-i. When the microwave power was 600 W, a mixture of nano-belts and microspheres was formed (Fig. 3 a and **b**), whereas when the microwave power was 700 W, a composite of nanoparticles and nanorods was formed (Fig. 3 c, **h**, **i**). When the microwave power was increased to 900 W, it led to the formation of thick rod structures (Fig. 3 d). Fig. 3 d, **e**, **f**, and **g** illustrate the effects of microwave pulses on the morphology of the final product. It was observed that the morphology of the product changed into nanoparticles as the microwave running time increased in each cycle. The SEM images of piezo-catalysts C10–C15 are shown in Fig. 4 a-i. An analysis of the effect of microwave times on the morphology of products revealed that when the microwave time was 3 min, a mixture of rods and nanoparticles formed (Fig. 3 c). As the microwave time was increased to 4 min, almost uniform nanoparticles with 20–40 nm in diameter and some with 150–200 nm in diameter were formed (Fig. 4a). By increasing the microwave time to 6 min, rods of 100–400 nm diameter were formed, as well as nanoparticles of 20–100 nm in diameter (Fig. 4 b and **c**). Comparison of SEM images of Fig. 4 a and Fig. 4 d, **e**, and **f** can provide insight into the effect of calcination temperature. A temperature of 400 °C was used for the calcination process in order to produce microspheres and nanorods. Increasing the calcination temperature to 550 °C resulted in the formation of uniform nanoparticles with a diameter of 20–40 nm, as well as some particles with a diameter of 150–200 nm. If the calcination temperature is increased to 700 °C, however, a slightly larger nanoparticle is formed (Fig. 4 f). In addition, calcination time could have a significant impact on the morphology of products. The results for calcination times of 3, 5, and 5 h are shown in Fig. 4 a, **g**, **h**, and **i**. As the calcination time was increased to 5 h, the morphology of catalysts became spherical nanoparticles. It was observed that very small nanoparticles were formed when the calcination time was 3 h (Fig. 4 g and **h**). As the calcination time was increased to 5 h (Fig. 4 a), nanoparticles became larger. While the calcination time was increased to 7 h, nanoparticles and rods were formed (Fig. 4 i).

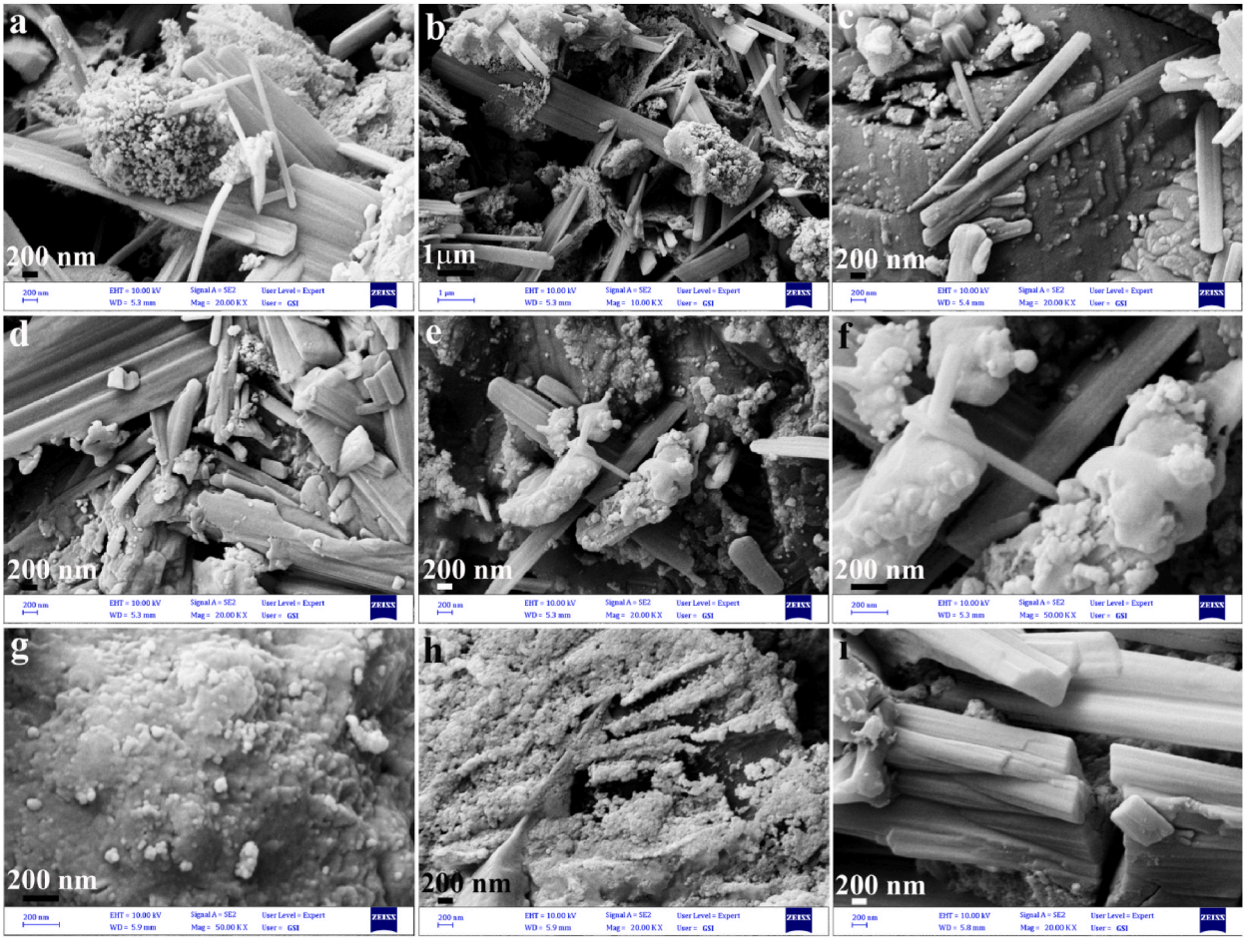

Fig. 3. SEM image of a, b) C1, c) C4, d) C3, e, f) C5, g) C6, and h, i) C7.

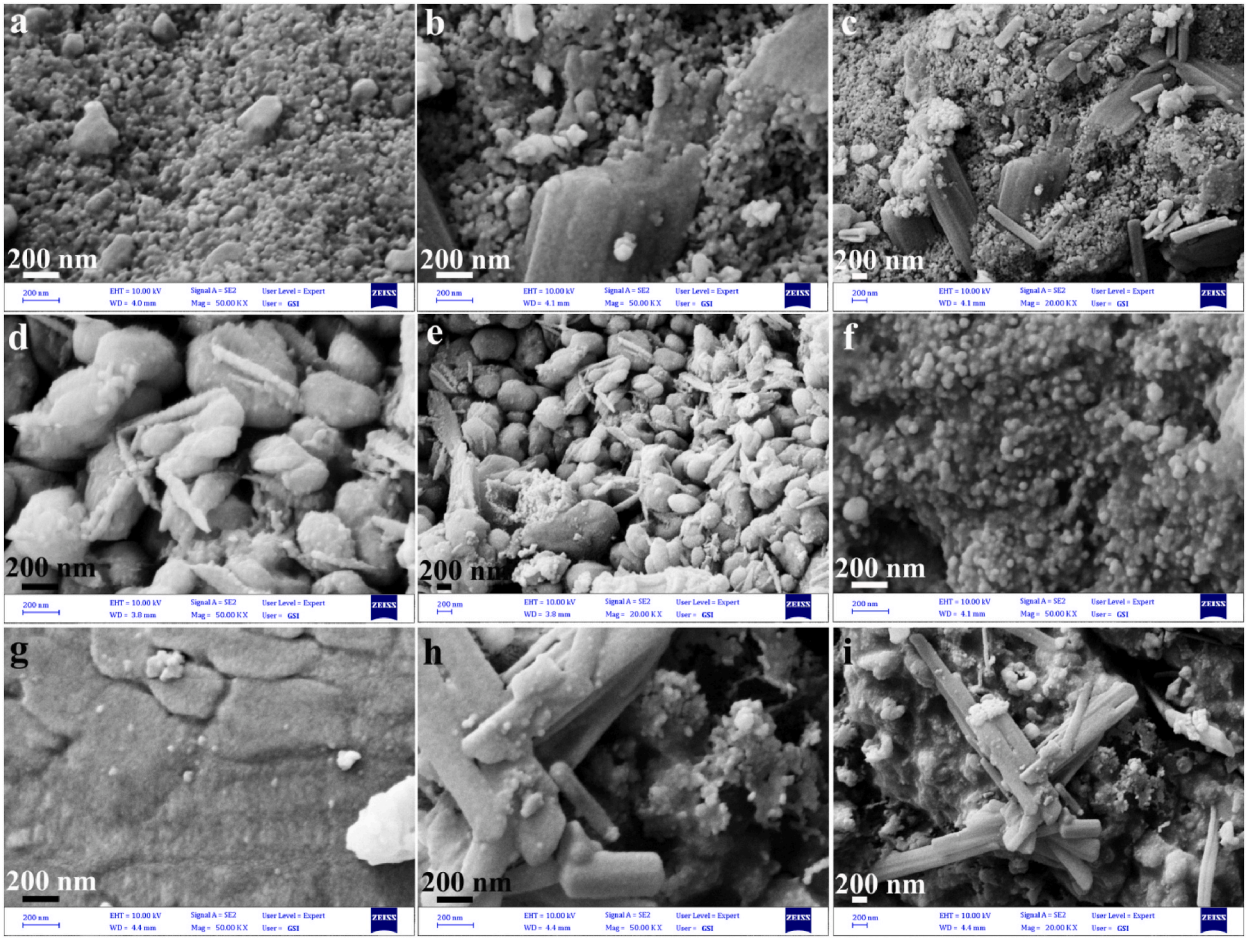

Fig. 4. SEM image of a) C10, b, c) C11, d, e) C12, f) C13, g) C14, and h, i) C15.

Additionally, EDX results confirm the successful synthesis of Ce_xO_y/SrO nanocomposites (Fig. 5 a and **b**). SEM images and XRD peaks indicate that the highest quality, uniform, and well-crystalline samples were obtained using 700 W microwave power for 5 min and 700 °C calcination time for 5 h. In the TEM image of sample C10 (Fig. 5 c), which was prepared under optimum experimental conditions, the spherical nanocomposite is clearly visible and confirms its morphology and size.

3.2. Piezo-desulfurization by prepared catalysts: effect of synthesis parameters on the desulfurization rate

The four steps below (eqs. (2)–(5)) have been explained about piezoelectric catalysis process and degradation mechanism;

$$Ce_xO_y/SrO\ NCS + force \rightarrow (Ce_xO_y/SrO\ NCS)\ (e^- + h^+) \quad (2)$$

$$O_2 + e^- \rightarrow {}^{\cdot}O_2^- \quad (3)$$

$$h+ + OH\text{-} \rightarrow {}^{\cdot}OH \quad (4)$$

$$h+/e^-/{}^{\cdot}OH/{}^{\cdot}O_2^- + sulfur \rightarrow oxidaized\ sulfur \quad (5)$$

All of the parameters that can make a change directly produce electrons and holes can affect the desulfurization rate [27]. Several studies have strongly indicated that nanomaterials, including nanowires (NWs) and nanoflowers (NFs), were commonly used in piezocatalysis [29–31]. It has been found that the piezoelectric properties of spherical $Pb(Zr_{0.52}Ti_{0.48})O_3$ are more significant than the morphology and structure of piezo-catalysis and that the free charges in piezoelectric materials play a primary role in piezoelectric catalysis [29]. However, the findings of this research confirm that due to the ease of structural deformation, nanomaterials such as Ce_xO_y/SrO nanocomposites have a greater piezoelectric potential than bulk particles.

A Ce_xO_y/SrO nanocomposites were successfully synthesized and then employed to desulfurize thiophene and dibenzothiophene as model fuels, as well as kerosene with 2000 ppm sulfur as a real fuel using ultrasonic to activate the piezo-catalyst. As illustrated in Fig. 6 and Table 3, as-prepared nanocomposite piezocatalysts were used for the desulfurization of TP, DBTP. The desulfurization

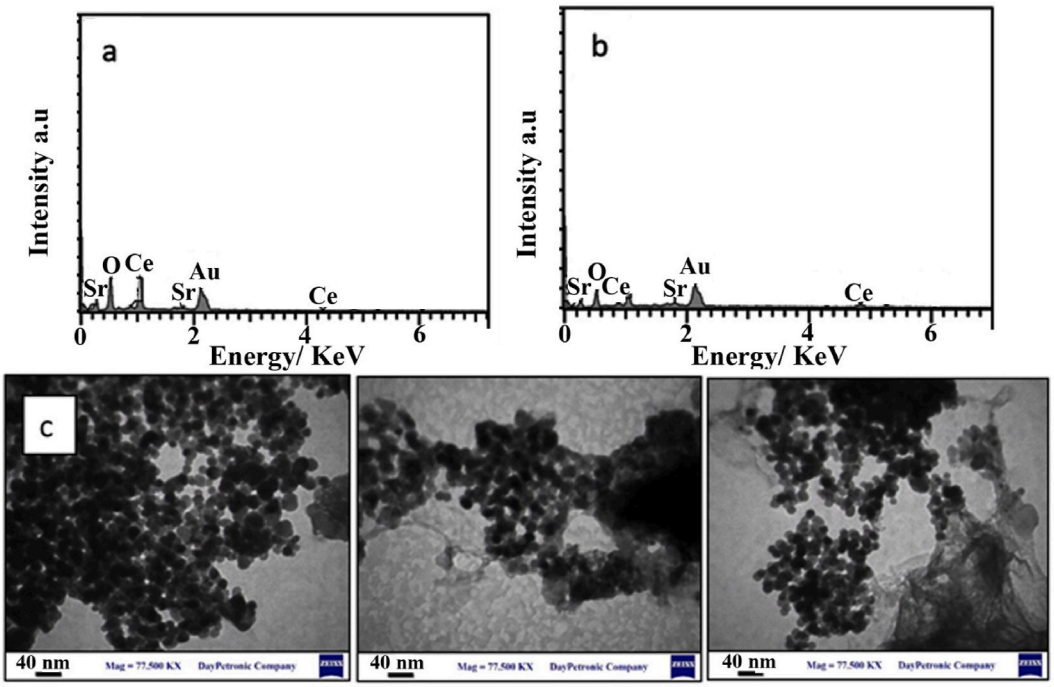

Fig. 5. A) EDX of sample C10, b) EDX of sample C13, c) TEM image of C10.

process was organized with 75 ppm of each catalyst dosage and using ultrasonic with the power of 320 W within 30 min. The shaking period was 15 min.

Maximum sulfur removal was observed in sample C13 with a uniform spherical and crystalline structure with the formula CeO_2/SrO. Desulfurization rates are 95.4 % and 97.3 % for TP and DBTP. Due to the small size of the particles and the uniform spherical morphology of the particles, the mechanical force coming from ultrasonic can meet all of the particles efficiently. 320 W is quiet

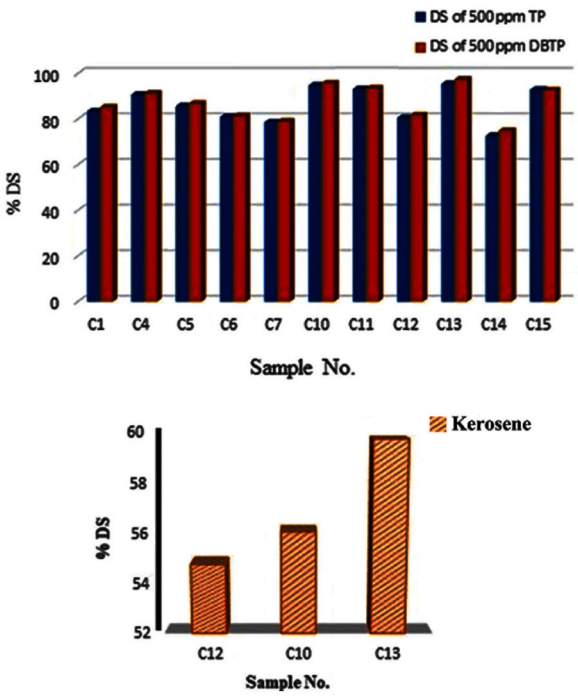

Fig. 6. Piezo-desulfurization results for TP, DBTP and Kerosene by using as-prepared nanocomposites as catalyst.

enough to polarize and create a built-in electric field in piezo-catalysts, which will separate the positive and negative charges when exposed to external mechanical forces. As a result, electrons and holes can be continuously separated and pass through the opposite surface via piezocatalytic redox reactions nonstop and continuously [32]. As part of the piezo-catalyst removal process, a number of parameters can affect the oxidative desulfurization rate. Using TP and DBTP as model fuels and kerosene as the real fuel, this research examined the effect of pH of the media, sulfur concentration, piezo-catalyst dosage, ultrasonic power and time, and shaking time on the piezo-desulfurization process.

3.3. Effect of piezo-catalyst dosage on the sulfur removal

TP and DBTP desulfurization rates have been investigated using C10 as a piezo-catalyst and different catalyst dosages of 10, 25, 50, 75, and 100 mg (Fig. 7 a). During 30 min of ultrasonic treatment with 320 W in power, the desulfurization rate of TP jumped from 57.7 % to 94.7 % when the catalyst dosage was raised from 10 mg to 75 mg. The most effective catalyst dosage was 75 mg, as upping the dosage from 75 mg to 100 mg resulted in a decrease in sulfur removal and produced only waste piezo-catalyst without any efficient sulfur removal. By increasing the amount of piezo-catalyst, it appears that the active site of the piezo-catalyst facing mechanical force to create electrons and holes has been decreased or saturated. Similar behavior was observed with DBTP as well. As a result of increasing the catalyst dosage from 10 ppm to 75 ppm, the desulfurization rate increased from 59.4 % to 95.6 %. However, once the catalyst dosage reached 100 mg, it decreased to 95.1 %.

3.4. Effect of sulfur content on the piezo-removal efficiency

For the purpose of studying the effect of sulfur content on desulfurization rate, a piezo-catalyst of C10 with a 75 mg dosage was selected. TP and DBTP concentrations of 100, 250, 500, 750, and 1000 ppm were studied for the effect of sulfur concentration (Fig. 7 b). In accordance with our expectations, the rate of desulfurization decreased with an increase in the concentration of TP and DBTP. The results in this study indicate that with the same amount of force derived from ultrasonic power, the determined number of electrons and holes can be produced. This can only affect the same amount of sulfur compounds. As the sulfur concentration increases, there will be insufficient superoxide to react with sulfur compounds, which can result in sulfur removal. According to these results, desulfurization rates decreased from 98.4 % to 99.1 % for 100 ppm TP and DBTP, respectively, to 51.9 % and 60.3 % respectively for 1000 ppm TP and DBTP.

3.5. Effect of pH on the piezo-removal of sulfur compound

The piezo desulfurization experiments were conducted at three different pH levels (4, 7, and 10), with the pH being adjusted to the desired level by adding 0.1 M H_2SO_4 and 0.1 M NaOH. At a pH of 4, adjusted with H_2SO_4, the chosen piezo-catalyst, C10, removed 97.5 % of 500 ppm TP and 99 % DBTP. In the presence of 500 ppm TP and DBTP at natural pH (7), the desulfurization rate was 94.7 % and 95.6 %, respectively (Fig. 7 c). After increasing pH to 10, which is adjusted with sodium hydroxide, the desulfurization rate decreased to 78.2 % and 80.7 %, respectively. Because H_2SO_4 was used to adjust the pH of the prepared piezo catalysts, they performed better in acidic media. Since H_2SO_4 is an oxidant, it facilitates the oxidation of sulfur compounds and increases the effectiveness of sulfur removal [33]. Another key parameter that affects piezo-desulfurization removal is the shaking time. This refers to the amount of time it takes to extract the oxidized sulfur compounds from the remaining complex into the DMS phase. When the shaking time was 60 s, 50.7 % and 57.1 % of oxidized TP and DBTP were transferred to DMS, respectively. As the time was increased to 5 min, these values increased to 68.7 % and 71.4 %, respectively, for oxidized TP and DBTP. There are also results presented for three more determined extraction times (15, 30, and 60 min) in Fig. 7 d. According to these results, 15 min is the optimum extraction time since a longer shaking time did not significantly affect the desulfurization process.

Table 3
Piezo-catalyst desulfurization results for as-prepared catalysts in 75 ppm catalyst dosage in 30 min with 320 ultrasonic power.

Sample	DS of 500 ppm TP	DS of 500 ppm DBTP
C1	83.4	85.1
C4	90.7	91.2
C5	85.6	86.7
C6	80.9	81.2
C7	78.5	78.9
C10	94.7	95.6
C11	93.1	93.4
C12	80.5	81.6
C13	95.4	97.3
C14	72.6	74.8
C15	92.8	92.6

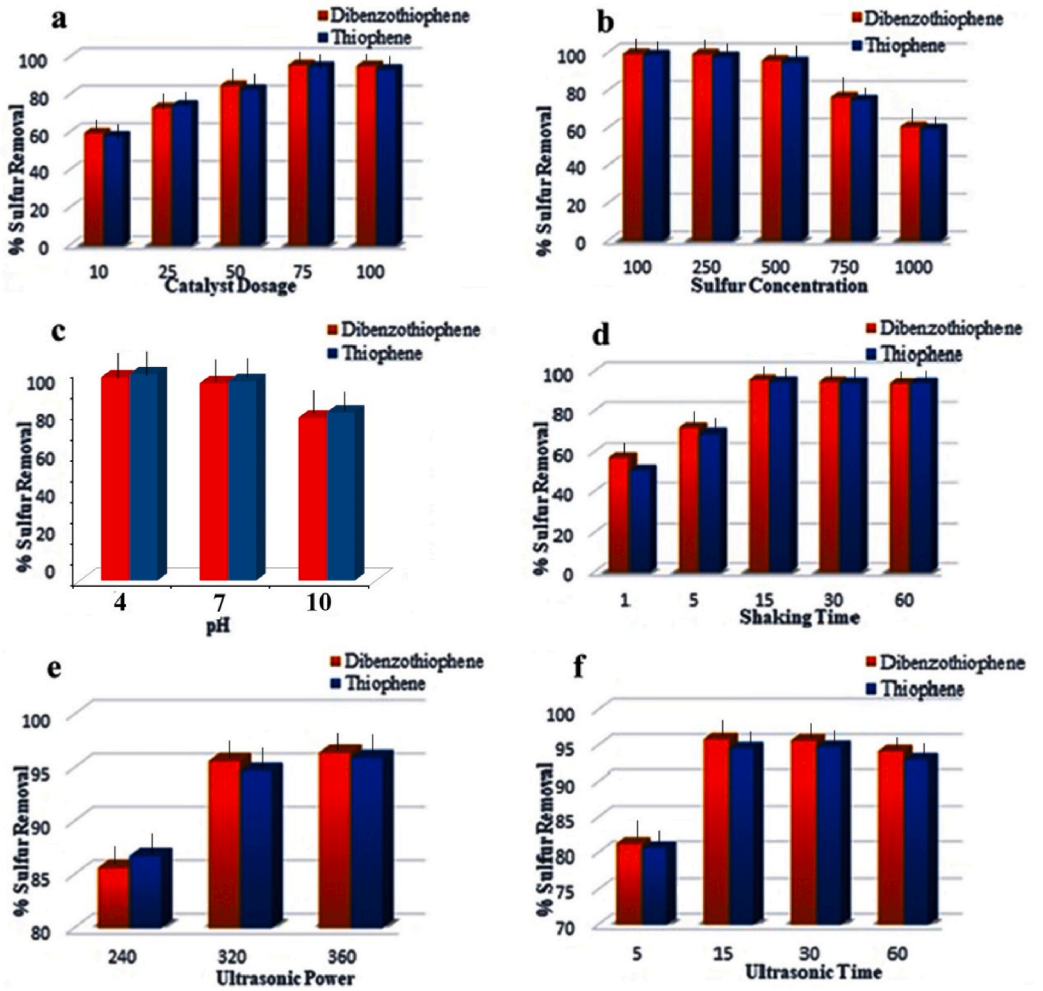

Fig. 7. Effect of operation parameters on the piezo-desulfurization rates: a) effect of catalyst dosage, b) effect of sulfur content, c) effect of pH of fuel, d) effect of shaking time e) effect of ultrasonic power, f) effect of ultrasonic time.

3.6. Effect of ultrasonic time and power on the piezo-removal efficiency

A high-frequency ultrasonic bath was used in this study to provide the mechanical force to the activated catalyst in a significant manner. Our previous work has shown some evidence to indicate how ultrasonic power affects the piezo catalyst's activity. We investigated that increasing ultrasonic power resulted in a decrease in degradation efficiency. We later found that this occurs because the temperature increases during sonication, and increasing the temperature significantly decreases efficiency [17,34]. Due to this observation, we kept the bath temperature constant at 30 ± 2 °C for all experiments. In the study, we found that the removal percentage for TP and DBTP went up from 86.7 % to 81.2 % when power was 240 W to 95.9 % and 96.4 % when power was 360 W (Fig. 7 e). By boosting sonication power at a constant temperature, mechanical force increased and desulfurization removal rates improved.

In the desulfurization test, ultrasonic power was constant at 320 W during the time intervals of 5, 15, 30, and 60 min (Fig. 7 f). This is because sonication plays a crucial role in the desulfurization process. The results indicated that 80.6 % of TP and 81.2 % of DBTP were removed during the first 5 min, confirming the rapid degradation of high-concentration TP and DBTP. The results of the study showed that by changing the ultrasonic time to 15 min and 30 min, respectively, the desulfurization rate of TP increased to 94.5 % and 94.7 %. According to the same ultrasonic time, the piezo-desulfurization rate for DBTP was 95.8% and 95.6%, respectively. TP degradation rates decrease to 92.9 after 30 min and to 94.1 after 60 min for DBTP. The results of this study indicate that 30 min of ultrasonic time is an ideal length of time, and almost all of the studies were conducted for 30 min.

3.7. Durability and reutilization of piezo-catalyst

Under the same experimental conditions, a piezo-catalyst was examined for its durability and reusability in the desulfurization of sulfur compounds (Fig. 8, Table 4). It was found that the removal efficiency for TP and DBTP decreased slightly after 11 cycles, while

that for real fuel decreased after 14 cycles. As a model catalyst, 75 ppm of C10 was used to remove 94.7 % of TP, 95.6 % of DBTP, and 56.1 % of kerosene in the first cycle during a 30 min ultrasonic process. In the removal of TP and DBTP after 11 cycles, C10 retained 79.4 % and 80.6 % of its piezo-desulfurization activity, respectively. Reusability of the catalyst is more promising for real fuel; even after 14 cycles it retained almost 75 % of its removal ability. Piezo-desulfurization for real fuel is significantly lower than for model fuel. This is due to the fact that kerosene contains 2000 ppm of sulfur, which is 4 times higher than model fuel.

3.8. Mechanism of active radical trapping for desulfurization by piezo-catalyst

Scavengers were used during ODS to recognize most active species during ODS. By adding free radical scavengers to the piezo catalytic system, we can probe the involvement of free radicals in the degradation process. If the addition of scavengers significantly reduces or inhibits the degradation of pollutants, it suggests that free radicals are crucial intermediates in the reaction pathway. This helps in elucidating the mechanism of pollutant degradation and identifying the key reactive species involved. It was found that piezo catalysts produced electrons and holes under ultrasonic conditions and that these electrons and holes could produce free radicals. These free radicals can oxidize sulfur compounds. In a reactor with a C10 piezo-catalyst, radical trapping experiments were conducted by adding IPA, Benzoquinone (BQ), and EDTA-2Na, which are scavengers of hydroxyl radicals (•OH), superoxide (O_2), and holes (h+). Fig. 9 and **schematic 1** illustrates the related results and mechanism of piezo-desulfurization. The formation of the superoxide radical plays a crucial role in the complete oxidation of TP and DBTP since the presence of BQ resulted in the reduction of the desulfurization degree from 94.7 % to 25 % and from 95.6 % to 21 % for TP and DBTP, respectively. In this experiment, ultrasonic waves can generate electrons and holes in the piezo-catalyst as a result of the external mechanical force created by ultrasonic waves. When electrons are generated, they can react with oxygen and produce radicals of oxygen. Besides electrons, generated holes can also react with H_2O to produce OH radicals or directly react with sulfur compounds, so the role of generated holes is equally critical in this mechanism, as adding EDTA-$_2$Na results in a decrease in desulfurization degree from 94.7 % to 36 % for TP and from 95.6 % to 29 % for DBTP, respectively. TP and DBTP conversions were not significantly altered by IPA addition, indicating that hydroxyl radicals (•OH) did not contribute significantly to piezo desulfurization.

3.9. Kinetic study of desulfurization

As a means of analysing the kinetic data of degradation and characteristic factors of desulfurization by piezo-catalyst, two conventional kinetic models were employed, namely pseudo-first-order and pseudo-second-order models. As a result of the pseudo-first-order model, the following formula (eq. (6)) can be found [35,36].

$$\mathrm{Ln}\ (qe - qt) = \ln qe - k_1 * t \tag{6}$$

Qe and qt represent the amount of sulfur compounds adsorbed at equilibrium (qe) and at different times (qt), calculated in mg/g, and k1 represents the pseudo-first-order model rate constant (1/min). It is possible to determine the values of qe and k1 by examining the intercept and slope of a linear plot of ln (qe −qt) versus t [37].

A table describing the pseudo-second-order model's kinetic parameters is also provided in Table 5 As can be seen in the table, the pseudo-second-order model [38,39] described in Equation below (eq. (7))

$$1/qt = 1/k_2 qe^{\,2} + 1/q_e \tag{7}$$

The study found that at different temperatures, different R^2 values were obtained for first-order and second-order kinetics. At 298 K, R^2 value for second-order kinetics was 0.948 while for first-order kinetics it was 0.942. Similarly, at 313 K and 333 K, R^2 values were 0.945 and 0.935 for first-order fitting and 0.959 and 0.969 for second-order fitting, respectively. Based on the results, it can be concluded that the reaction follows the second-order kinetic, specifically in the case of piezo degradation desulfurization by SrO/CexOy nanocomposites. Fig. 10a displays the average desulfurization of 500 parts per million total petroleum hydrocarbons (TPH) in the presence of sample C10 as a piezo-catalyst at different temperatures: 298 K, 313 K, and 333 K over a given period of time. As the reaction temperature increased, the piezo-desulfurization also increased. This trend could be explained by the fact that the temperature rise led to increased solubility of a sulfur compound in the solvent phase and increased the sulfide content, which in turn enhanced the reaction between the catalyst and the sulfur compound. Additionally, the oxidation of sulfide to sulfoxide and sulfoxide is endothermic, and increasing the reaction temperature shifts the equilibrium in the positive direction.

The second order rate constant's activation energy was found to be 3.824 Kj/mole, while the Arrhenius Constant for the second order reaction was determined to be 0.0236 mol^{-1}. Sec^{-1} (Fig. 10b). Beside, Table 6 compared the results of this new method with pervious methods.

4. Conclusion

As a result of our study, highly efficient piezo-catalysts have been introduced as promising nanomaterials for replacing previous desulfurization methods at room temperature using a mechanical force. As-prepared spherical nanocomposites consisting of CeO_2, referred to as cerianite and SrO, with cubic phase structures, were effective in removing up to 95 % of sulfur compounds in model fuels with 500 ppm sulfur content and 59.7 % in high sulfur content fuels with 2000 ppm sulfur content within 30 min. The Ce_xOy/SrO nanocomposites exhibited promising reusability, with a minor reduction in removal efficiency after 11 cycles for TP and DBTP and 14

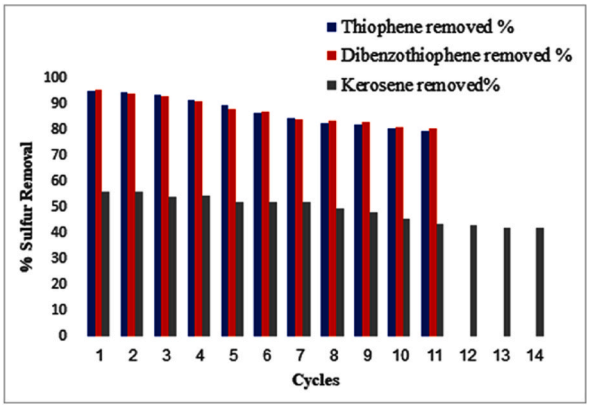

Fig. 8. (e) Reusability performance of as-prepared piezo-catalyst, sample C10 for Thiophene, Dibenzothiophene and Real fuel (Kerosene) at 30 ± 2 °C.

Table 4
Reutilization results of catalyst in piezo-desulfurization of TP, DBTP, and real fuel (Kerosene).

Cycle	Thiophene removed %	Dibenzothiophene removed %	Kerosene removed%
1	94.7	95.6	56.1
2	94.3	94.1	55.8
3	93.2	92.9	54
4	91.4	90.7	54.3
5	89.6	88.1	52
6	86.3	86.7	51.9
7	84.6	84.1	51.8
8	82.4	83.6	49.6
9	81.7	82.9	48
10	80.6	81.1	45.6
11	79.4	80.6	43.8
12			43.1
13			42.3
14			42.2

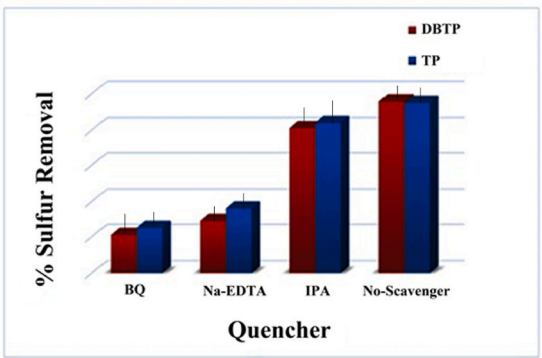

Quencher	Thiophene	Dibenzothiophene
BQ	25	21
Na-EDTA	36	29
IPA	84	81
No Scavenger	94.7	95.6

Fig. 9. Free radical trapping experiments of h+ (Na-EDTA),·OH (IPA) and·O_2.

Table 5
Kinetic Parameters for pseudo-first and pseudo-second-order model for different Temperature (SrO–Ce_2O_3).

		Temperature (K)		
Kinetic models	**Parameters**	**298**	**313**	**333**
Pseudo-First-Order	q_e (mg. g^{-1})	94.5	96.1	96.3
	K_1 (min^{-1})	0.311	0.342	0.368
	R^2	0.942	0.935	0.945
Pseudo-Second-Order	q_e (mg. g^{-1})	102.0	103.5	103.6
	K_2 (g. mg^{-1}. min^{-1})	0.0050	0.0055	0.0059
	R^2	0.948	0.959	0.969

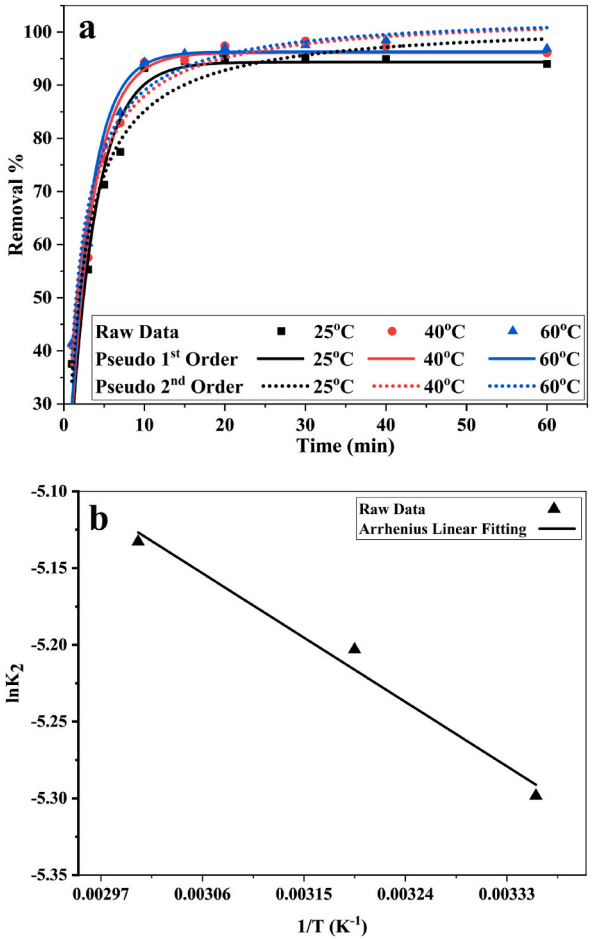

Fig. 10. A) Average desulfurization of 500 ppm TP in presence of sample C10 as piezo-catalyst at different temperatures. b) Kinetic rate constant vs Temperature.

Table 6
Comparing the desulfurization efficiency of this work with pervious methods.

	Catalyst	Method	Removal yield (%)	Ref.
1	FWF@PbO@PVA	CODS	97	[40]
2	Fe6W18O70⊂CuFe2O4	CODS	98	[41]
3	Fe2W18Fe4@FeTiO3	CODS	97	[42]
4	Cu-SPOM@PbO@PVA	CODS	97	[43]
5	15%Ag/Fe3O4/graphene	Photocatalytic desulfurization	94.5	[44]
6	CexOy/SrO nanocomposite	PDS	97.3	This work

cycles for kerosene. To gain a better understanding of the actual desulfurization behavior during piezo-desulfurization, a hole, hydroxyl radical, and superoxide scavenger were utilized to identify the mechanism of the piezo-desulfurization reaction and the role of various piezo reactive species. It was observed that the reactivity of these piezo-generated reactive species continuously increased from superoxide radicals to holes (h+) to hydroxyl radicals (.OH). Based on the kinetic results, it can be inferred that the reaction follows the second order with a rate constant of K = 0.0050. Moreover, the thermodynamic outcomes revealed that the oxidation of sulfide to sulfoxide and sulfoxide is endothermic. The second order rate constant's activation energy was found to be 3.824 Kj/mole, while the Arrhenius Constant for the second order reaction was determined to be 0.0236 mol^{-1}. Sec^{-1}

Data availability

All data generated or analyzed during this study are included in this published article (and its Supplementary Information files).

CRediT authorship contribution statement

Karwan M. Rahman: Methodology. **Omid Amiri:** Writing – review & editing, Writing – original draft, Supervision, Conceptualization. **Sangar S. Ahmed:** Writing – review & editing, Methodology, Formal analysis. **Savana J. Ismael:** Methodology. **Noor S. Rasul:** Writing – review & editing, Methodology. **Karukh A. Babakrb:** Methodology. **Mahnaz Dadkhah:** Writing – review & editing, Writing – original draft. **Mohammed A. Jamal:** Methodology.

Declaration of competing interest

The authors declare that they have no known competing financial interests or personal relationships that could have appeared to influence the work reported in this paper.

Acknowledgements

Authors are grateful to the council of University of Cihan-Erbil to support this work.

References

[1] I.V. Babich, J.A. Moulijn, Science and technology of novel processes for deep desulfurization of oil refinery streams: a review, Fuel 82 (2003) 607–631.
[2] D. Jha, M.B. Haider, R. Kumar, W.G. Shim, B. Marriyappan Sivagnanam, Batch and continuous adsorptive desulfurization of model diesel fuels using graphene nanoplatelets, J. Chem. Eng. Data 65 (2020) 2120–2132.
[3] N.Y. Dzade, N.H. de Leeuw, Adsorption and desulfurization mechanism of thiophene on layered FeS(001), (011), and (111) surfaces: a dispersion-corrected density functional theory study, J. Phys. Chem. C 122 (2018) 359–370.
[4] A. Tanimu, K. Alhooshani, Advanced hydrodesulfurization catalysts: a review of design and synthesis, Energy Fuel. 33 (2019) 2810–2838.
[5] J. Bai, X. Li, A. Wang, R. Prins, Y. Wang, Hydrodesulfurization of dibenzothiophene and its hydrogenated intermediates over bulk MoP, J. Catal. 287 (2012) 161–169.
[6] I. Shafiq, S. Shafique, P. Akhter, M. Ishaq, W. Yang, M. Hussain, Recent breakthroughs in deep aerobic oxidative desulfurization of petroleum refinery products, J. Clean. Prod. 294 (2021) 25731.
[7] J. He, Y. Wu, P. Wu, L. Lu, C. Deng, H. Ji, et al., Synergistic catalysis of the PtCu alloy on ultrathin BN nanosheets for accelerated oxidative desulfurization, ACS Sustain. Chem. Eng. 8 (2020) 2032–2039.
[8] C.M. Becker, M. Marder, E. Junges, O. Konrad, Technologies for biogas desulfurization - an overview of recent studies, Renew. Sustain. Energy Rev. 159 (2022) 112205.
[9] Y. Zhuo, Y. Han, Q. Qu, J. Li, C. Zhong, D. Peng, Characteristics of low H2S concentration biogas desulfurization using a biotrickling filter: performance and modeling analysis, Bioresour. Technol. 280 (2019) 143–150.
[10] X. Tang, J-y. Yuan, J. Li, Y. Zhang, T. Hu, Alkylation desulfurization of FCC gasoline catalyzed by pyridine ionic liquid, J. Fuel Chem. Technol. 43 (2015) 442–448.
[11] Y. Shiraishi, K. Tachibana, T. Hirai, I. Komasawa, A novel desulfurization process for fuel oils based on the formation and subsequent precipitation of S-alkylsulfonium salts. 3. Denitrogenation behavior of light oil feedstocks, Ind. Eng. Chem. Res. 40 (2001) 3390–3397.
[12] I. Shafiq, S. Shafique, P. Akhter, G. Abbas, A. Qurashi, M. Hussain, Efficient catalyst development for deep aerobic photocatalytic oxidative desulfurization: recent advances, confines, and outlooks, Catal. Rev. 12 (2021) 1–46.
[13] T. Zhang, X. Chen, B. Ding, Z. Ding, Y. Wang, H. Qiu, et al., Deep oxidative desulfurization of model fuels catalyzed by subnanosized Ti oxoclusters, Energy Fuel. 36 (2022) 1402–1416.
[14] M. Seredych, T.J. Bandosz, Removal of dibenzothiophenes from model diesel fuel on sulfur rich activated carbons, Appl. Catal. B Environ. 106 (2011) 133–141.
[15] S.R. Anton, H.A. Sodano, A review of power harvesting using piezoelectric materials (2003–2006), Smart Mater. Struct. 16 (2007) R1.
[16] K.-S. Hong, H. Xu, H. Konishi, X. Li, Direct water splitting through vibrating piezoelectric microfibers in water, J. Phys. Chem. Lett. 1 (2010) 997–1002.
[17] O. Amiri, K. Salar, P. Othman, T. Rasul, D. Faiq, M. Saadat, Purification of wastewater by the piezo-catalyst effect of PbTiO(3) nanostructures under ultrasonic vibration, J. Hazard Mater. 394 (2020) 122514.
[18] Z. Liang, C.-F. Yan, S. Rtimi, J. Bandara, Piezoelectric materials for catalytic/photocatalytic removal of pollutants: recent advances and outlook, Appl. Catal. B Environ. 241 (2019) 256–269.
[19] J-j. Li, F. Zhou, X-d. Tang, N. Hu, Deep desulfurization of kerosene by electrochemical oxidation generating Na2FeO4, Energy Fuel. 30 (2016) 8091–8097.
[20] Sh Lan, J. Feng, Y. Xiong, Sh Tian, Sh Liu, L. Kong, Performance and mechanism of piezo-catalytic degradation of 4-chlorophenol: finding of effective piezo-dechlorination, Environ. Sci. Technol. 51 (2017) 6560–6569.
[21] J. Long, T. Ren, J. Han, N. Li, D. Chen, Q. Xu, H. Li, J. Lu, Heterostructured BiFeO3@CdS nanofibers with enhanced piezoelectric response for efficient piezocatalytic degradation of organic pollutants, Separ. Purif. Technol. 290 (2022) 120861.
[22] L. Shi, Ch Lu, L. Chen, Q. Zhang, Y. Li, T. Zhang, X. Hao, Piezocatalytic performance of Na0.5Bi0.5TiO3 nanoparticles for degradation of organic pollutants, J. Alloys Compd. 895 (2022) 162591.
[23] O. Amiri, A. Abdalrahman, G. Jangi, H.A. Ahmed, S.H. Hussein, M. Joshaghani, R.Z. Mawlood, M. Salavati-Niasari, Convert mechanical energy to chemical energy to effectively remove organic pollutants by using PTO catalyst, Separ. Purif. Technol. 283 (2022) 120235.

[24] W. Yang, G. Guo, Z. Mei, Y. Yu, Deep oxidative desulfurization of model fuels catalysed by immobilized ionic liquid on MIL-100(Fe), RSC Adv. 9 (2019) 21804–21809.
[25] T. Liu, L. Wang, X. Lu, J. Fan, X. Cai, B. Gao, et al., Comparative study of the photocatalytic performance for the degradation of different dyes by ZnIn2S4: adsorption, active species, and pathways, RSC Adv. 7 (2017) 12292–12300.
[26] J.T. Schneider, D.S. Firak, R.R. Ribeiro, P. Peralta-Zamora, Use of scavenger agents in heterogeneous photocatalysis: truths, half-truths, and misinterpretations, Phys. Chem. Chem. Phys. 22 (2020) 15723–15733.
[27] G. Nie, Y. Yao, X. Duan, L. Xiao, S. Wang, Advances of piezoelectric nanomaterials for applications in advanced oxidation technologies, Current Opinion in Chemical Engineering 33 (2021) 100693.
[28] K. S. Hong, H. Xu, H. Konishi, X. Li, Piezoelectrochemical effect: a new mechanism for azo dye decolorization in aqueous solution through vibrating piezoelectric microfibers, J. Phys. Chem. C 116 (2012) 13045–13051.
[29] Y. Feng, L. Ling, Y. Wang, Z. Xu, F. Cao, H. Li, et al., Engineering spherical lead zirconate titanate to explore the essence of piezo-catalysis, Nano Energy 40 (2017) 481–486.
[30] M.-H. Wu, J.-T. Lee, Y.J. Chung, M. Srinivaas, J.-M. Wu, Ultrahigh efficient degradation activity of single-and few-layered MoSe2 nanoflowers in dark by piezo-catalyst effect, Nano Energy 40 (2017) 369–375.
[31] M.J. Gordon, T. Baron, F. Dhalluin, P. Gentile, P. Ferret, Size effects in mechanical deformation and fracture of cantilevered silicon nanowires, Nano Lett. 9 (2009) 525–529.
[32] Y. Wang, Y. Xu, S. Dong, P. Wang, W. Chen, Z. Lu, et al., Ultrasonic activation of inert poly(tetrafluoroethylene) enables piezocatalytic generation of reactive oxygen species, Nat. Commun. 12 (2021) 3508.
[33] W. Zhang, J. Yang, Y. Hu, X. He, X. Zhu, R.V. Kumar, et al., Effect of pH on desulphurization of spent lead paste via hydrometallurgical process, Hydrometallurgy 164 (2016) 83–89.
[34] K.A. Babakr, O. Amiri, L.J. Guo, M. A Rashi, P.H. Mahmood, Kinetic and thermodynamic study in piezo degradation of methylene blue by SbSI/Sb(2)S(3) nanocomposites stimulated by zirconium oxide balls, Sci. Rep. 12 (2022) 15242.
[35] Y. Fan, Kinetics and mechanism analysis of CO2 adsorption on LiX@ZIF-8 with core shell structure, Powder Technol. 399 (2022) 117090, 2022.
[36] H. Wang, H. Shen, C. Shen, Y-n. Li, Z. Ying, Y. Duan, Kinetics and mechanism study of mercury adsorption by activated carbon in wet oxy-fuel conditions, Energy Fuel. 33 (2019) 1344–1353.
[37] S. Deng, R. Wang, H. Xu, X. Jiang, J. Yin, Hybrid hydrogels of hyperbranched poly (ether amine) s (hPEAs) for selective adsorption of guest molecules and separation of dyes, J. Mater. Chem. 22 (2012) 10055–10061.
[38] F. Duan, C. Chen, G. Wang, Y. Yang, X. Liu, Y. Qin, Efficient adsorptive removal of dibenzothiophene by graphene oxide-based surface molecularly imprinted polymer, RSC Adv. 4 (2014) 1469–1475.
[39] A.S. Bhatt, P.L. Sakaria, M. Vasudevan, R.R. Pawar, N. Sudheesh, H.C. Bajaj, et al., Adsorption of an anionic dye from aqueous medium by organoclays: equilibrium modeling, kinetic and thermodynamic exploration, RSC Adv. 2 (2012) 8663–8671.
[40] N. Khalafi, M.A. Rezvani, V. Jafarian, Facile synthesis of new hybrid nanocomposite sandwich-type polyoxometalate@lead (II) oxide@polyvinyl alcohol as an efficient and reusable amphiphilic nanocatalyst for ODS of real fuel, Adv. Powder Technol. 34 (2023) 103877.
[41] M.A. Rezvani, A. Imani, Ultra-deep oxidative desulfurization of real fuels by sandwich-type polyoxometalate immobilized on copper ferrite nanoparticles, Fe6W18O70 ⊂ CuFe2O4, as an efficient heterogeneous nanocatalyst, J. Environ. Chem. Eng. 9 (2021) 105009.
[42] M.A. Rezvani, S. Khandan, Synthesis and characterization of new sandwich-type polyoxometalate/nanoceramic nanocomposite, Fe2W18Fe4@FeTiO3, as a highly efficient heterogeneous nanocatalyst for desulfurization of fuel, Solid State Sci. 98 (2019) 106036.
[43] M.A. Rezvani, N. Khalafi, Deep oxidative desulfurization of real fuel and thiophenic model fuels using polyoxometalate-based catalytic nanohybrid material, Mater. Today Commun. 22 (2020) 100730.
[44] O. Amiri, F. Beshkar, S.S. Ahmed, B.W. Hamad, P.H. Mahmood, A.A. Dezaye, Magnetically-driven Ag/Fe3O4/graphene ternary nanocomposite as efficient photocatalyst for desulfurization of thiophene under visible-light irradiation, Int. J. Hydrogen Energy 46 (2021) 19913–19925.